A CMOS Z-AXIS CAPACITIVE ACCELEROMETER WITH COMB-FINGER SENSING

Huikai Xie* and Gary K. Fedder*†
*Department of Electrical and Computer Engineering and †The Robotics Institute
Carnegie Mellon University, Pittsburgh, PA 15213-3890, USA
Email: xie@ece.cmu.edu; Tel: (412) 268-6607

ABSTRACT

This paper reports the first design and experimental results of a z-axis accelerometer that utilizes sidewall capacitance change of multi-conductor comb fingers. The accelerometer has a fully differential capacitive bridge interface and its fabrication is compatible with standard CMOS processes. The frequency response of the accelerometer is characterized both electrically and optically and about 9.3 kHz resonant frequency is measured, which matches MEMCAD simulation within 15%. Measured sensitivity is 0.5 mV/g with less than -40 dB cross-axis sensitivity, noise floor 6 mg/rtHz, and linear range from -27g to 27g.

INTRODUCTION

Interdigitated comb fingers have been widely used for actuation and frequency tuning [1][2]. In principle, they can also be used for displacement or acceleration detection in all three directions. Integrated tri-axial accelerometers have such advantages as smaller size and less cost than the combination of three discrete single-axis accelerometers. Analog Devices has successfully developed polysilicon surface micromachining lateral-axis comb-finger accelerometers [3]. However, z-axis comb-finger accelerometers are not easy to make because of parasitic capacitance to the substrate in polysilicon processes and electrical isolation difficulties in bulk micromachining processes. Selvakumar *et al.* reported a capacitive z-axis accelerometer using comb-finger sensing [4]. They use a dissolved-wafer process to make polysilicon movable fingers (rotors) and stationary fingers (stators) separately anchored on a glass substrate and thus reduce the parasitic capacitance to the substrate.

Based on a high-aspect-ratio CMOS micromachining process [5], a new capacitive-sense method is developed which solves the parasitic capacitance and insulation problems. The CMOS micromachining process includes a maskless post process and is completely compatible with standard CMOS processes. In the process, metal layers from previous CMOS processes are used as etching mask. As a result, the interface circuitry is automatically protected by the top metal layer, and microstructures consist of up to three metal layers which are insulated by oxide. By choosing different metal layers as an etching mask, beams with different thickness can be obtained simultaneously. The cross-section after the final step of the process is illustrated in Figure 1

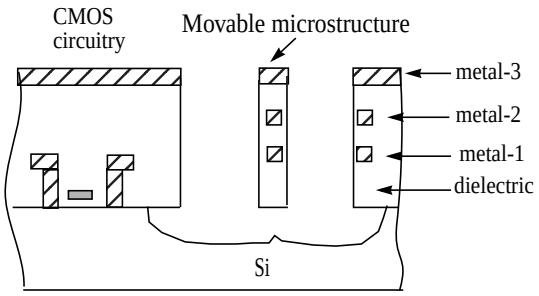

Figure 1: Cross-section of CMOS micromachining process

where the released microstructure is between 15 μm and 35 μm above the silicon substrate, which effectively eliminates the parasitic capacitance to the substrate. Moreover, the multiple conductor layers existing in the microstructures provide high flexibility for wiring so that a fully differential capacitive-bridge interface can be easily implemented. Meanwhile, the inherited out-of-plane curling due to residual stress gradient in the composite structural layers can also be partially solved using a self-aligned design [6].

In earlier work, a CMOS lateral-axis accelerometer has been made by using the CMOS micromachining process [6]. The three metal layers in every comb finger are electrically connected together, so that the comb fingers function the same way as homogenous polysilicon counterparts. However, metal layers in multi-conductor comb fingers can also be selectively interconnected to form two sidewall capacitors between comb fingers whose capacitances change with z-displacement in opposite directions. That is the basic idea of the proposed z-axis

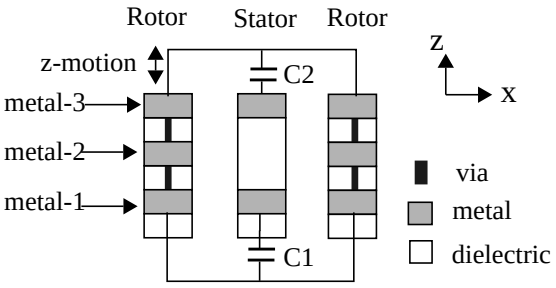

(a) Cross-section of a pair of comb fingers

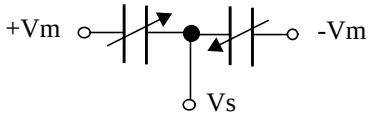

(b) Equivalent capacitive-bridge

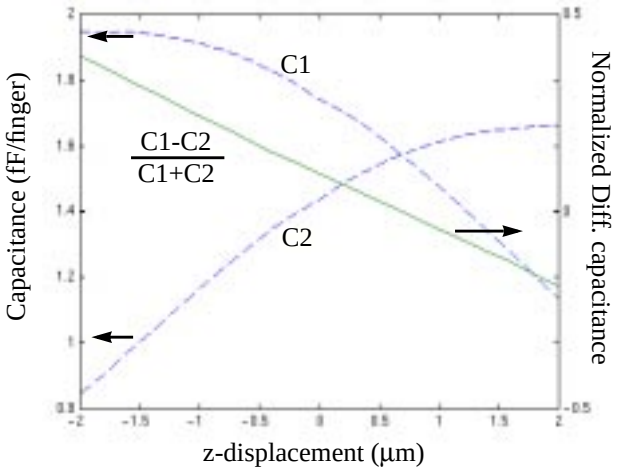

(c) Calculated capacitance vs. z-displacement (50 μm engaged length are assumed)

Figure 2: Principle of the z-displacement capacitive-sensing through comb-fingers

accelerometer. We will present the structure design, field simulation, thermomechanical and modal analyses, and electrical and optical measurement results. In this paper, we only consider 3-metal-layer CMOS process. The same concept can be applied to an arbitrary number of metal layers.

OPERATIONAL PRINCIPLE

Capacitance change is often used as a measure of displacement in microaccelerometers. The sensitivity in one direction depends on both the capacitance gradient and the mechanical stiffness in that direction. The cross-section of a pair of multi-conductor comb-fingers is shown in Figure 2(a). The stator finger is constructed of metal-1 and metal-3 layers which are insulated by oxide, while the rotor finger includes three metal layers which are electrically connected together. Two sidewall capacitors C1 and C2 are formed. When the rotor finger moves up or down, for example, by an external acceleration, C1 and C2 will change value in opposite directions. As an electrical circuit, C1 and C2 form a differential capacitive half-bridge, as shown in Fig. 2(b). If balanced modulation voltages +/-*Vm* are applied, the output signal *Vs* is expressed as

$$V_S = \frac{C1 - C2}{C1 + C2} V_m \qquad (1)$$

Figure 2(c) shows the simulation results of C1, C2 and their differential changes with z-displacement using the Maxwell 2D field simulator [7]. Although C1 and C2 are not linear with z-displacement, the normalized differential capacitance changes almost linearly with z-displacement from -2 μm to +2 μm. If the rotor fingers are attached to a proof mass and a spring, the output voltage is

$$V_S = \frac{ma}{k} V_m \frac{d}{dz} G(z) \qquad (2)$$

where G(z) = (C1-C2)/(C1+C2), *m* is the mass of the proof mass, *k* is the stiffness of the spring in the z-axis, and *a* is an external acceleration in the z direction. We can rewrite (2) as

$$Vs / Vm = Ka \qquad (3)$$

where K is the sensitivity with units of V/g/V. The sensitivity depends on the spring, proof mass, amplifier, but is constant as long as the system is operating in its linear range.

Note that the wide linear displacement range (+/-2 μm) is remarkable, since large dynamic range can be achieved without compromising sensitivity or bandwidth. Very low cross-sensitivity is expected in this configuration because C1 and C2 are the summation of the capacitances formed in both sides of the stator and the stiffness of the lateral axes is designed to be much bigger than that of the z-axis.

The differential capacitance curve in Fig.2(c) is not symmetric, i.e., G(z) ≠0 at z = 0. Instead, a d.c. offset of 0.6 μm exists. The d.c. offset can be adjusted by a prescribed displacement of 0.6 μm realized by properly designing the curl matching frame described in the next section.

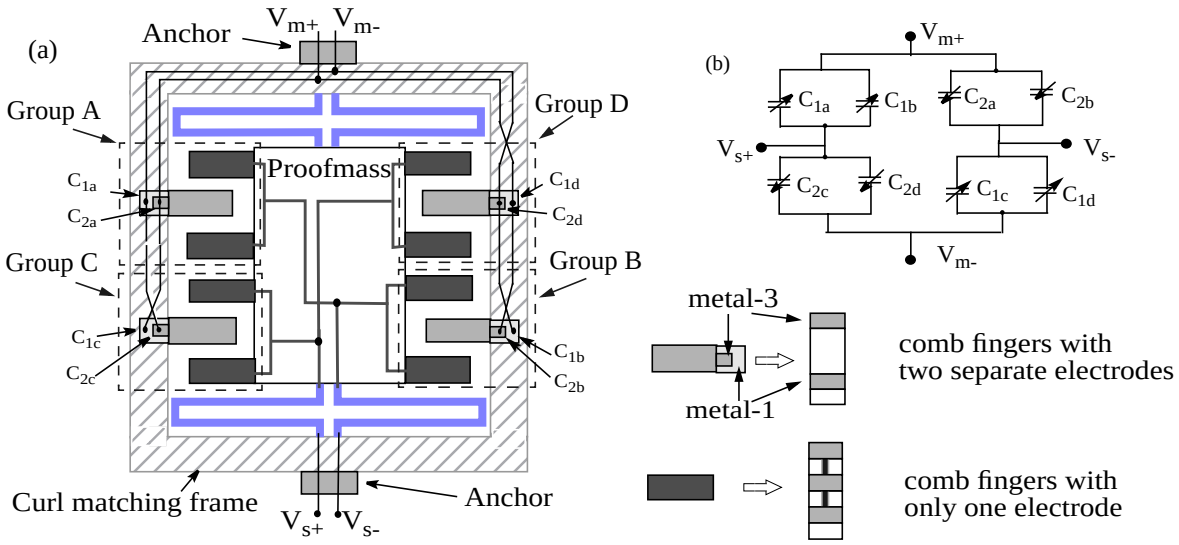

Figure 3. Topology design and wiring configuration of the z-axis accelerometer. (a) Schematic of the top view of the layout with a common-centroid configuration. (b) Equivalent full-bridge differential capacitive interface.

STRUCTURE DESIGN & SIMULATION

The multi-conductor layer structure provides a high flexibility for wiring which makes it easy to implement full-bridge differential capacitive interfaces. The comb fingers are divided into 4 groups as shown in Figure 3(a). All comb fingers have exactly the same cross-section as shown in Fig.2(a). The only difference is the wiring. In Groups A and B, the top metal layer is connected to Vm+, and the bottom metal layer to Vm-. In Groups C and D, the wiring is reversed. In this way, we obtain a full-bridge differential capacitive interface as shown in Fig.3(b). Moreover, the four groups constitute a common-centroid configuration which reduces the lateral-axis sensitivity and the influence of process variations.

As we mention above, the CMOS micromachining process can make structures of different thicknesses at different locations by simply choosing different metal layers as the etching mask. In order to further reduce the cross-sensitivity, we design the spring to be covered only by metal-1 as shown in Figure 4. After release, the thickness of the spring will be much thinner that the rest of

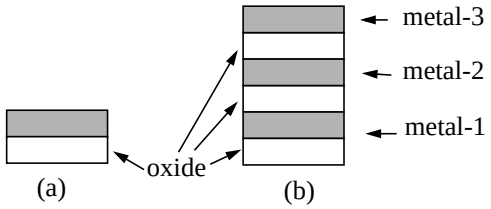

Figure 4. Cross-sections at different locations of a structure. (a) Spring; (b) Proof mass and frame.

the structure, making the spring soft in the z direction. Since the structure is made of multiple material layers, the residual stress gradient makes structures curl up, especially for thin beams with only metal-1 on the top [8]. In order to obtain a better understanding, thermomechanical simulation is performed in MEMCAD 4.5 [9]. Two simplifications are made to reduce the number of elements: 1) the holes on the structure for etch release are eliminated; 2) only two pairs of comb fingers are used to model the curl matching behavior. The result is shown in Figure 5 which indicates that the spring curls much more than the rest of the structure. The rotor fingers match the stator fingers well through the curl matching frame.

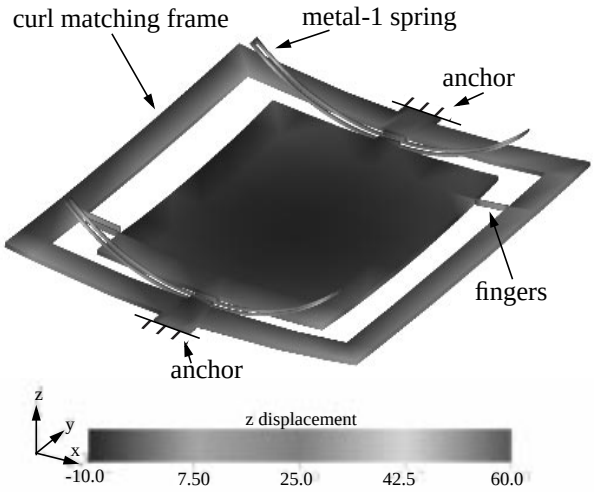

Figure 5. Thermomechanical simulation of the z-axis accelerometer

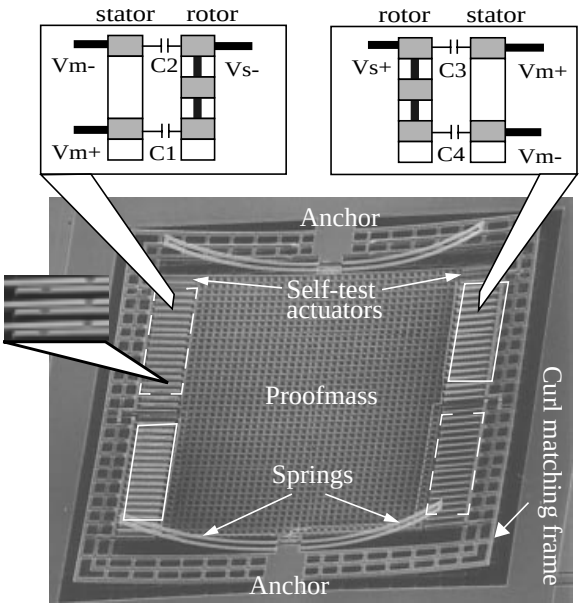

Figure 6. Top view of a released z-axis accelerometer

FABRICATION

The accelerometer is fabricated in the Hewlett-Packard 0.5 µm CMOS process followed by a two-step maskless process. First, CHF_3 is used to etch the oxide anisotropically. Mask metals and the silicon substrate are then exposed. Second, SF_6 is used to etch silicon isotropically. Proper timing is important to achieve both complete release and maximum protection of vias. A released accelerometer is shown in Figure 6. The size of the device including the on-chip buffers and preamplifier is about 0.5 mm x 0.7 mm. The two sets of fingers outlined with a white solid line are electrically connected, as are the other two sets outlined with a white dashed line. Schematic cross-sections are shown at the top of the SEM. The spring beams curl up about 55 µm at their ends due to the residual stress and thermal coefficient mismatch in the embedded layers inside the beams. However, the stator and rotor fingers align very well (<0.5 µm vertically and <0.1 µm laterally) through a curl matching frame, which matches within 15% with the simulation result shown in Figure 5. There is one extra pair of comb fingers at each corner of the proofmass. These comb fingers are electrically separated from the sense comb fingers. They are used as electrostatic actuators for self-test and/or DC offset adjustment.

MEASUREMENT

The test set-up is shown in Figure 7. The packaged accelerometer is mounted on a shaker table whose motion is monitored by a high accuracy reference accelerometer, and a spectrum analyzer (HP4395A) is used to analyze the output signal. A 200 Hz sinusoidal excita-

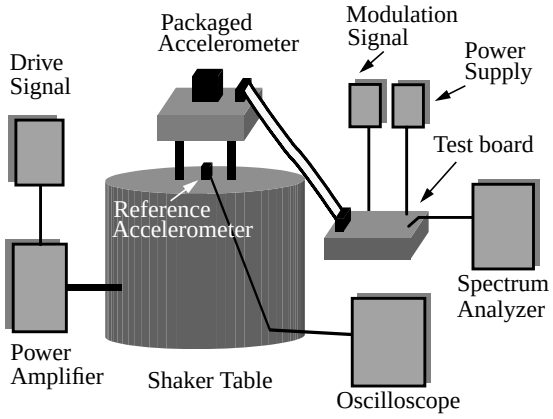

Figure 7. The experimental set-up for z-axis accelerometer test

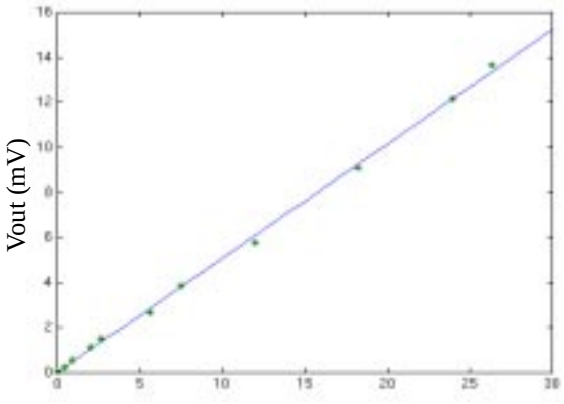

Figure 8. Dynamic response measured at 200Hz using a shaker table

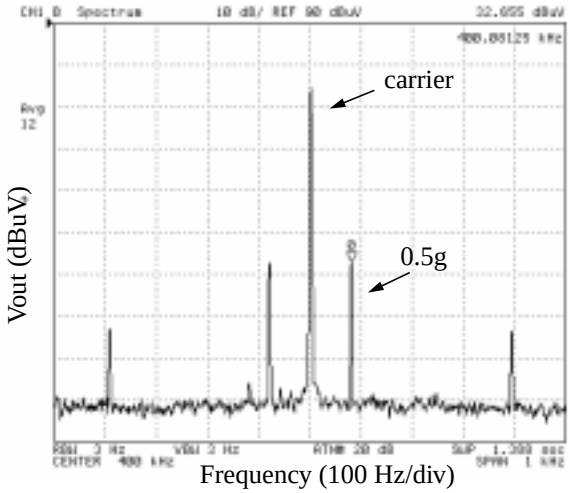

Figure 9. Spectrum of the output signal when a 0.5g 80Hz external acceleration is applied

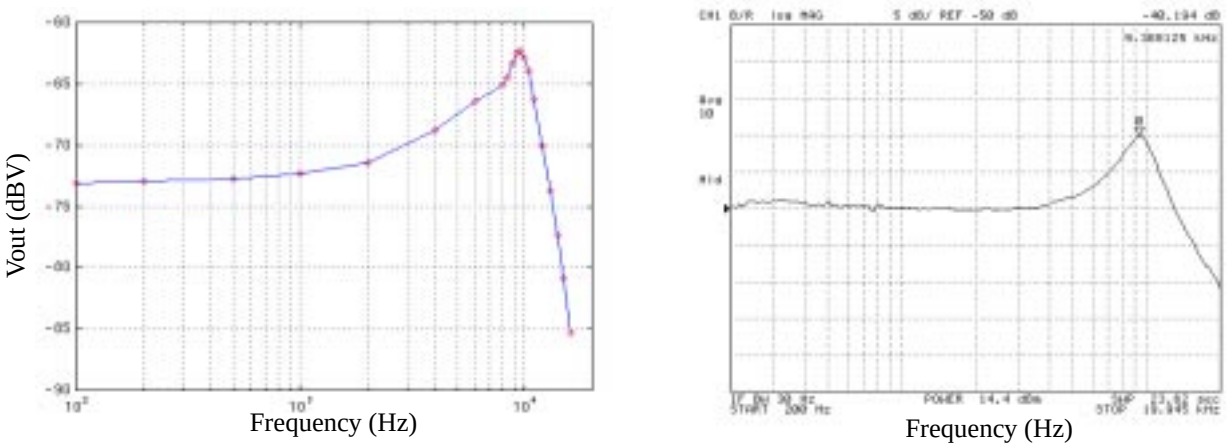

(a) Capacitive sensing by comb fingers

(b) Measured by the optical interferometer

Figure 10: Frequency response of the accelerometer

tion signal is used to drive the shaker table and the modulation signal is set to a 800 mV 400 kHz sine wave. The measurement result for dynamic range is shown in Figure 8. The response is still linear when the amplitude of the external acceleration increases to 27 g, which is the maximum limit of the shaker table. The theoretical linear range is +/-600 g because of the wide linear range (+/-2 μm) of the differential capacitance change with z-displacement. The overall sensitivity is 0.5 mV/g. A typical spectrum of the output signal is shown in Figure 9 where a 0.5 g 80 Hz excitation acceleration is applied. The measured noise floor is 6 mg/rtHz which is one order higher than the calculated Brownian noise. The increased noise level is probably due to the test circuits and vibrations existing in the test environment.

The frequency response of the accelerometer is characterized both electrically and optically as shown in Figure 10. For electrical characterization, the accelerometer is excited by applying a sinusoidal voltage to the self-test actuators. In order to reduce the effect of the feedthrough of the excitation signal, a sinusoidal signal with zero d.c. bias is used to generate force at double the input electrical frequency. The frequency response detected through the sensing comb fingers is shown in Figure 10(a). In order to explore the actual motion, a Michaelson optical interferometer system is employed. The schematic of the optical set-up is shown in Figure 11(a). A LED is used as the light source instead of a laser to improve the image quality. A typical interference image is shown in Figure 11(b). A photodetector combined with a network analyzer is used to conduct frequency sweeping and obtain

(a)

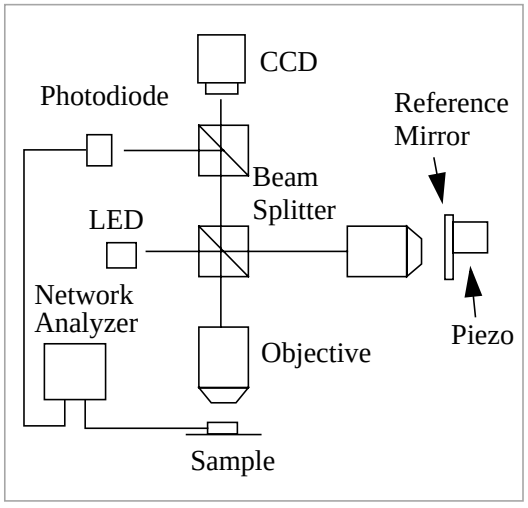

(b)

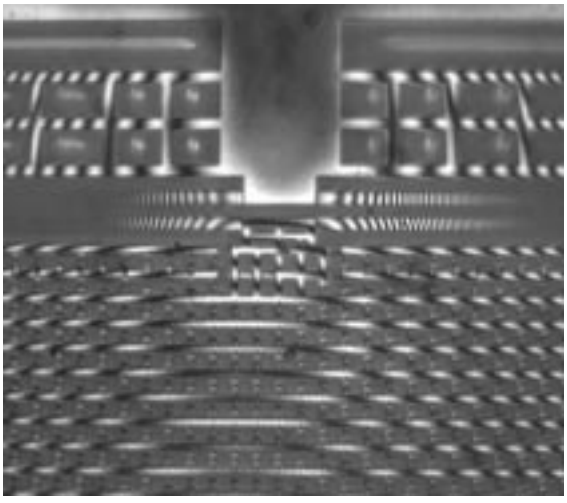

Figure 11. Optical measurement using a Michaelsoninterferometer. (a) Optical set-up; (b) Interference pattern around the upper anchor (each fringe occurs at 310 nm vertical displacement).

transfer function directly. The measured frequency response is shown in Figure 10(b). The two different measurements give close resonant frequencies of 9.2 kHz for capacitive and 9.4 kHz for optical detection. The resonant frequency predicted by MEMCAD simulation is 10.1 kHz. The 10% error is attributed to fabrication process variations and the simplification of the model, e.g., modeling the perforated proof mass as a solid plate. The measurement results are summarized in Table 1. Note that the Q factor is only about 3, which results from the squeeze-damping of the proofmass.

Table 1: Parameters of the accelerometer

	Designed	Measured
Dimension	500x700 μm^2	-
Resonant frequency	10.1kHz	9.4kHz
Quality factor in air	-	3
Sensor sensitivity	0.75mV/g/V	0.5mV/g/V
Cross-sensitivity	-55dB	<-40 dB
Linear range	+/-600g	+/-27g
Noise floor	0.6 mg/rtHz (Brownian; Q=3)	6 mg/rtHz

CONCLUSION

A new method for vertical capacitive sensing is proposed in this paper. Based on the method, the first design of CMOS z-axis comb-finger accelerometers was successfully fabricated and characterized. The device has several advantages including low cost, large dynamic range, on-chip integrated signal processing circuits, and realization of integrated tri-axial accelerometers when combined with existing lateral accelerometers. The same concept for vertical comb-finger sensing can be applied to comb-finger vertical actuation.

In the next generation, the asymmetry of the upper and lower capacitances will be compensated by alternating the interconnects of the metal layers in the stator and rotor fingers. The vertical curling of the springs made of only metal-1 must be reduced through design.

ACKNOWLEDGEMENT

The authors thank Hao Luo for circuit design, Hasnain Lakdawala for MEMCAD simulation, Dr. Lars Erdmann for optical measurement and Suresh Santhanam for chip release and SEMs. This research was sponsored by DARPA under the AFRL, Air Force Materiel Command, USAF, under agreement F30602-97-2-0323.

REFERENCES

[1] V.P. Jaecklin, C. Linder, N.F. de Rooij, J.M. Moret, "Micromechanical comb actuators with low driving voltage", *Journal of Micromechanics and Microengineering*, vol.2, no.4, p. 250-5

[2] Ki Bang Lee, Young-Ho Cho, "Frequency tuning of a laterally driven microresonator using an electrostatic comb array of linearly varied length", *Proceedings of International Solid State Sensors and Actuators Conference (Transducers '97)*, Chicago, IL, USA; 16-19 June 1997, p113-16

[3] Analog Devices, "ADXL05 +/-1g to +/- 5g single chip accelerometer with signal conditioning." Datasheet, 1995, Norwood, MA 02062.

[4] A. Selvakumar, K. Najafi, "A high-sensitivity z-axis capacitive silicon microaccelerometer with a torsional suspension", Journal of Microelectromechanical Systems, vol.7, no.2, p. 192-200

[5] G.K. Fedder, S. Santhanam, M.L. Reed, S.C. Eagle, D.F. Guillou, M. Lu, L.R. Carley, "Laminated high-aspect-ratio microstructures in a conventional CMOS process," *Sensors and Actuators A*, vol.A57, no.2, p.103-110

[6] G. Zhang, H. Xie, L.E. Derosset, G.K. Fedder, "A lateral capacitive CMOS accelerometer with structural curl compensation", *Proceedings of 12th International Workshop on Micro Electro Mechanical Systems (MEMS'99)*, Orlando, FL, USA; 17-21 Jan. 1999, p606-611.

[7] Maxwell 2D field simulation, Version 1.9.04, Copyright 1984-1997, Ansoft Corporation

[8] M. S.-C. Lu, X. Zhu, and G. K. Fedder, "Mechanical Property Measurement of 0.5 mm CMOS Microstructures," Proc. MRS 1998 Spring Meeting, Symposium N, San Francisco, CA, April 13-17, 1998.

[9] MEMCAD User Guide, Microcosm Technologies Inc., 201 Willesden Dr., Cary, NC 27513. http://www.memcad.com